

# REPORT DOCUMENTATION PAGE

*Form Approved*  
*OMB No. 0704-0188*

Public reporting burden for this collection of information is estimated to average 1 hour per response, including the time for reviewing instructions, searching existing data sources, gathering and maintaining the data needed, and completing and reviewing this collection of information. Send comments regarding this burden estimate or any other aspect of this collection of information, including suggestions for reducing this burden to Department of Defense, Washington Headquarters Services, Directorate for Information Operations and Reports (0704-0188), 1215 Jefferson Davis Highway, Suite 1204, Arlington, VA 22202-4302. Respondents should be aware that notwithstanding any other provision of law, no person shall be subject to any penalty for failing to comply with a collection of information if it does not display a currently valid OMB control number. **PLEASE DO NOT RETURN YOUR FORM TO THE ABOVE ADDRESS.**

<b>1. REPORT DATE (DD-MM-YYYY)</b> 16-06-2010		<b>2. REPORT TYPE</b> Technical Paper		<b>3. DATES COVERED (From - To)</b>	
<b>4. TITLE AND SUBTITLE</b>  <b>Shear Force in Radiometric Flows</b>				<b>5a. CONTRACT NUMBER</b>	
				<b>5b. GRANT NUMBER</b>	
				<b>5c. PROGRAM ELEMENT NUMBER</b>	
<b>6. AUTHOR(S)</b> Natalia E. Gimelshein & Sergey F. Gimelshein (ERC, Inc.); Andrew D. Ketsdever (AFRL/RZSA); Nathaniel P. Selden (USC)				<b>5d. PROJECT NUMBER</b>	
				<b>5f. WORK UNIT NUMBER</b> 50260542	
				<b>8. PERFORMING ORGANIZATION REPORT NUMBER</b>  AFRL-RZ-ED-TP-2010-290	
<b>7. PERFORMING ORGANIZATION NAME(S) AND ADDRESS(ES)</b>  Air Force Research Laboratory (AFMC) AFRL/RZSA 10 E. Saturn Blvd. Edwards AFB CA 93524-7680				<b>10. SPONSOR/MONITOR'S ACRONYM(S)</b>	
<b>9. SPONSORING / MONITORING AGENCY NAME(S) AND ADDRESS(ES)</b>  Air Force Research Laboratory (AFMC) AFRL/RZS 5 Pollux Drive Edwards AFB CA 93524-7048				<b>11. SPONSOR/MONITOR'S NUMBER(S)</b> AFRL-RZ-ED-TP-2010-290	
<b>12. DISTRIBUTION / AVAILABILITY STATEMENT</b>  Approved for public release; distribution unlimited (PA #10299).					
<b>13. SUPPLEMENTARY NOTES</b> For presentation at the 27 <sup>th</sup> International Symposium on Rarefied Gas Dynamics, Monterey, CA, 10-15 July 2010.					
<b>14. ABSTRACT</b>  The impact of the radiometer vane thickness and edge geometrical shape on the total radiometric force is examined numerically solving the ES BGK model kinetic equation. The flow of argon over a single vane and a multi-vane configurations is considered in the range of Knudsen numbers from 0.02 to 1. The shear force is found to reduce the total radiometric force for most vane configurations. It is shown that the change in the vane shape may offset the losses due to the shear force in the multi-vane geometry.					
<b>15. SUBJECT TERMS</b>					
<b>16. SECURITY CLASSIFICATION OF:</b>			<b>17. LIMITATION OF ABSTRACT</b>	<b>18. NUMBER OF PAGES</b>	<b>19a. NAME OF RESPONSIBLE PERSON</b>
<b>a. REPORT</b>	<b>b. ABSTRACT</b>	<b>c. THIS PAGE</b>			Mr. Marcus Young
<b>Unclassified</b>	<b>Unclassified</b>	<b>Unclassified</b>	SAR	7	<b>19b. TELEPHONE NUMBER</b> <i>(include area code)</i> N/A

# Shear Force in Radiometric Flows

Natalia E. Gimelshein<sup>\*</sup>, Sergey F. Gimelshein<sup>\*</sup>, Andrew D. Ketsdever<sup>†</sup> and Nathaniel P. Selden<sup>\*\*</sup>

<sup>\*</sup>*ERC, Inc, Edwards AFB, CA 93524*

<sup>†</sup>*Propulsion Directorate, Edwards AFB, CA 93524*

<sup>\*\*</sup>*University of Southern California, Los Angeles, CA 90089*

**Abstract.** The impact of the radiometer vane thickness and edge geometrical shape on the total radiometric force is examined numerically solving the ES BGK model kinetic equation. The flow of argon over a single vane and a multi-vane configurations is considered in the range of Knudsen numbers from 0.02 to 1. The shear force is found to reduce the total radiometric force for most vane configurations. It is shown that the change in the vane shape may offset the losses due to the shear force in the multi-vane geometry.

**Keywords:** Radiometric force, shear, ES-BGK equation

**PACS:** 51.10.+y

## INTRODUCTION

The kinetic theory of gases predicts the existence of a force on a surface that has the length scale comparable to the gas mean free path, when there is a temperature gradient near that surface. This force is usually called radiometric. The simplest device making use of the radiometric force consists of a planar vane whose sides are kept at different temperatures. There are several mechanisms that contribute to radiometric force exerted by gas on a radiometer vane. One of them was explained as early as 1879 by Reynolds [1], who suggested a kinetic theory explanation based on the fact that the molecules colliding with the hot side leave with an increased velocity relative to those colliding with the cold side. This leads to a larger momentum flux change on the hot side, and results in the motion of the vanes with the hot side trailing. This is in fact a free molecular approximation of the radiometric effect, and the associated force may be referred to as area force.

At about the same time as Reynolds, Maxwell [2] also showed that an unbalanced force exists near the edge of the heated side of the vane, where the heat flow in the gas is non-uniform. Almost fifty years later, Einstein [3] presented a simple theory, according to which a force exerted on the vane is proportional to its perimeter. This edge dependence of the vane force has found partial confirmation in experimental work [4], where the force was shown to depend on perimeter, although the dependence is weaker than the Einstein's prediction. More recently, an analytic expression for the radiometric force was derived [5] that has both pressure and shear components. The latter one, often ignored in earlier studies, is produced by the interaction of gas with the lateral surface of the vane. The results of work [5], where the shear force was predicted to act from hot to cold side, thus increasing the total radiometric force, was in fact found to contradict the numerical results obtained by different kinetic approaches [6, 7, 8]. Both the direct simulation Monte Carlo method and the numerical solution of model kinetic equation, as well as the combined ES-BGK/DSMC approach, showed that the shear force on a rectangular radiometer would decrease the total force.

Either positive [5] or negative [6], the shear force is expected to be noticeably smaller than the pressure force on the working side of the radiometer, assuming that the radiometer is sufficiently thin. Although the magnitude of the shear force, which generally depends on the vane thickness, is noticeably smaller than the area and the edge forces exerted on the working sides of the radiometer [9], its contribution is expected to grow with gas pressure. Even more important, the shear force may be a significant contributor in multi-vane configurations, where the vanes are closely packed and there is a transpiration flow between the cold and hot sides of the radiometer. The main objective of this work is the numerical analysis of the shear contribution from the lateral sides of the vanes to the total radiometric force in a single and multi-vane radiometers immersed in rarefied gas. The effect of vane separation, thickness and geometry, as well as surface temperature and gas pressure, is investigated with a finite volume solver SMOKE [6] based on the solution of ES-BGK model kinetic equation.

## FLOW CONDITIONS

The study of the contribution of shear forces on the lateral side of a radiometer vane is conducted in pure argon for two radiometer configurations. In the first one, a flow over an 11 cm diameter circular vane is computed, immersed in a 3 m diameter and 3 m long cylindrical chamber. Note that the baseline radiometer vane corresponds to that previously studied experimentally [6]. The flow is axially symmetric, and the chamber size was chosen large enough to avoid possible impact of chamber walls on the force distribution over the vane. Similar to [6], the vane temperature is set to 420 K at the hot side, and 395 K at the cold side. A step-wise temperature distribution is assumed on the lateral side of the vane, which is divided into three equal parts with temperatures of 420 K (adjacent to the hot side of the vane), 407.5 K (middle part), and 395 K (adjacent to the cold side). A uniform chamber wall temperature of 300 K is assumed. In order to study the effect of radiometer geometry, the vane thickness is varied between 0.5 and 1.5 cm, and, in addition to the right-angled configuration, the angles of 60° and 120° between hot side plane and the lateral side are considered. The above configurations are examined in a wide range of pressures from 0.02 Pa to 1.2 Pa, to capture the pressure range where the radiometric force is maximum.

It has been found recently [10] that the efficiency (force versus mass at a given radiometer area) of a radiometer configuration may be drastically increased if instead of a single vane, multiple smaller vanes (sub-vanes) are used, separated by gaps comparable to the sub-vane size. Maximum radiometric force from a multi-vane configuration may be orders of magnitude larger than the maximum force of a single vane configuration comprising the same area, provided the size of the sub-vanes is small enough. The problem that arises for any multi-vane configuration, though, is related to strong force degradation caused by the shear forces when the working sides of the sub-vanes become comparable in size to the lateral sides. The question therefore arises if it would be possible to offset the losses from the shear forces by gains in the pressure forces through changing the geometrical shape of sub-vane edges. The geometry modification is expected to impact the thermal transpiration from the cold to the hot side, and thus may change the balance between pressure and shear forces.

To investigate the possibility of increasing the total force of a multi-vane configuration through the shear force reduction, a two-dimensional argon flow over a seven vane geometry is studied here, with the sub-vane length of 10 cm and thickness varied from 0.5 cm to 1.5 cm. The sub-vane separation is 7 cm, and the size of the chamber is 1 m by 1 m. The angle between the hot side plane and the lateral side is varied between 60° and 120°. Similar to the single-vane configuration, the hot and cold sides of the vanes are 420 K and 395 K, respectively, while the chamber wall is assumed to be 300 K.

## NUMERICAL APPROACH

The importance in radiometric flow of kinetic phenomena such as temperature jump, thermal creep, and viscous heating, as well as significant impact of flow non-equilibrium, results in inapplicability of shear stress and heat flux assumptions used in the Navier-Stokes equations and many analytic approaches, and leaves the computational methods of the kinetic gas theory as the only alternative. The DSMC method [11], which is currently the principal kinetic approach for modeling rarefied gas flows, is extremely time consuming for low speed flows due to long time to reach steady state and low signal-to-noise ratio. A plausible numerical alternative is a deterministic solution of one of the simplified forms of the Boltzmann equation, known as model kinetic equations. Two of the better known model kinetic equations, the Bhatnagar-Gross-Krook (BGK) [12] and the ellipsoidal statistical (ES) [13] kinetic models, use a non-linear relaxation term instead of the full Boltzmann collision integral. Despite a simpler collision term, both models possess the same collision invariants as the Boltzmann equation.

The existence of numerically efficient implicit integration schemes for these equations [14] allows for accurate numerical modeling of microflows at a reasonable computational cost. In this work, a finite volume solver SMOKE [6] has been used to deterministically solve the ES model kinetic equation. SMOKE is a parallel code based on conservative numerical schemes developed in [14]. The code has both two-dimensional and axisymmetric capabilities. A second order spatial discretization was utilized along with implicit time integration. Fully diffuse reflection with complete energy accommodation was applied at the radiometer vanes and chamber walls. A symmetry plane was set at the lower boundary. The grid convergence was achieved by increasing the number of spatial nodes and points in the velocity space. The latter one was (18,18,12) for the results presented below, and the number of spatial cells varied from 5,000 to 50,000 depending on the chamber size. The radiometric force on the vane was calculated through the integration of the velocity distribution functions of the incoming and outgoing molecules.

## SINGLE VANE CONFIGURATION

The first configuration considered in this work is a circular vane with varied thickness and edge shape. The impact of vane thickness on gas flow around the vane is shown in Fig. 1 (left) for a gas pressure of 0.954 Pa, where the radiometric force is near its maximum. Note that only part of the computational domain is shown in order to provide more detail in the vicinity of the vane. General structure of the flow does not change when the vane thickness is increased: there are two vortices, a small vortex at the cold side (counterclockwise for the upper half of the flow), and a large vortex that initiates at the hot side and recirculates gas in the entire chamber. The intensity of the vortices, though, significantly decreases when vane thickness increases. For example, the gas velocity in front of the cold side decreases from about 1.5 m/s for a vane thickness  $W = 0.5$  cm to 1 m/s for  $W = 1.5$  cm. The flow structure for two slanted geometries is shown in Fig. 1 (right). Here, the angle  $\alpha$  of the lateral wall is measured for its uppermost position, with  $\alpha = 0$  coinciding with the positive direction of the Y axis (see Fig. 1 (left)). In this case, the values of  $\alpha$  smaller than  $90^\circ$  correspond to the geometries with the hot side smaller than the cold side. It is seen that there is a significant increase in the magnitude of flow velocities at the lateral wall for  $\alpha = 60^\circ$ . For the  $\alpha = 120^\circ$ , there is another vortex formed at the lateral side of the vane.

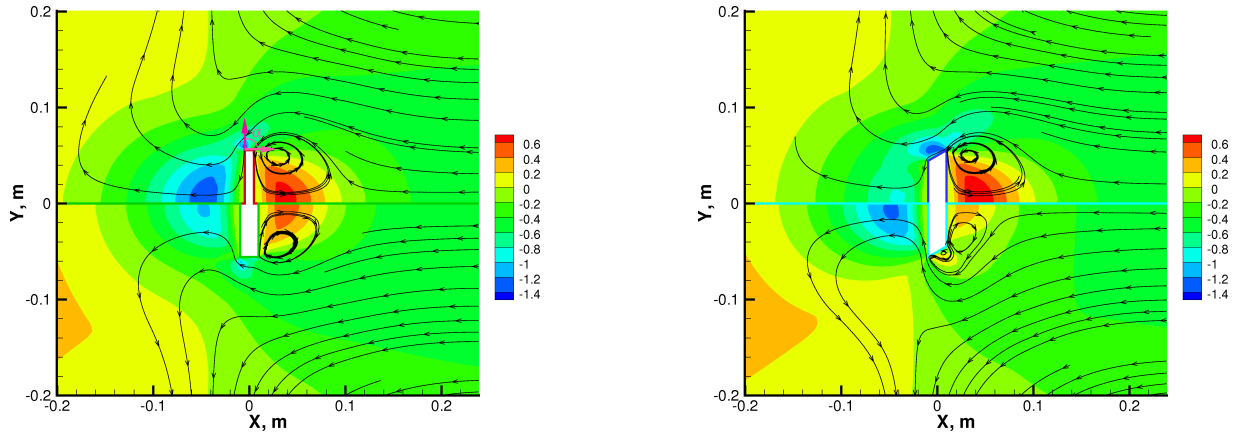


**FIGURE 1.** Axial velocity and streamlines for  $\alpha = 90^\circ$ ,  $W = 0.5$  cm (left top),  $\alpha = 90^\circ$ ,  $W = 1.5$  cm (left bottom),  $\alpha = 60^\circ$ ,  $W = 1.5$  cm (right top) and  $\alpha = 120^\circ$ ,  $W = 1.5$  cm (right bottom).

The important property that impacts the distributed and total forces on the vane is gas pressure. Pressure flowfields for the four geometries considered above are shown in Fig. 2. Comparing two straight edged vanes with different thickness, note that for both geometries, the gas pressure is elevated near the edge of the radiometer vane. This has been previously shown and explained in [7]. It was mostly attributed to the lower temperatures and therefore higher gas density and correspondingly higher mass flux from the regions adjacent to the side walls. Interesting to note that the increase in the vane thickness results in somewhat smaller gas pressures, especially near the hot side. This indicates that the pressure difference between the hot and cold sides is influenced by the gas recirculation. A thicker vane makes gas recirculation and associated thermal transpiration less efficient, and is therefore expected to decrease the total radiometric force. The slanted edge geometry (both  $\alpha = 60^\circ$  and  $\alpha = 90^\circ$ ) visibly decreases gas pressure around the vane, although this decrease is observed both at the cold and hot sides of the vane, and thus the total effect of the gas force may only be obtained after a quantitative analysis of the contributions of different sides of the vane.

The radiometric force directed from hot to cold side along the X axis is listed in Table 1 for various vane geometries and gas pressures. Here, pressure force  $F_p$  combines the difference between the pressure forces on the hot and cold sides and the projection of the pressure force on the lateral sides to X axis (zero for  $\alpha = 90^\circ$ ),  $F_s$  is the projection of the shear force on the lateral side of the vane to X axis, and  $F_{tot}$  is the total force which is the sum of the above two forces. As expected, for the lowest pressure, where the flow is nearly free molecular, the shear force on the lateral side of the vane for  $\alpha = 90^\circ$  is negligible, and the total radiometric force is mostly defined by the pressure difference on the hot and cold sides. The shear force contribution for  $\alpha = 90^\circ$  increases with pressure, and always acts in the direction opposite to the total radiometric force.

For  $\alpha = 60^\circ$ , the force in the lowest pressure case is almost 25% lower than for  $\alpha = 90^\circ$ . However, this starts to change when gas pressure increases. While the contribution of the pressure forces become smaller, the shear force strongly increases with pressure for  $\alpha = 60^\circ$ . The shear force increase results in a larger total radiometric force not only compared to the straight vane of the same thickness, but also to a thinner straight vane. Note that  $\alpha = 60^\circ$  is not

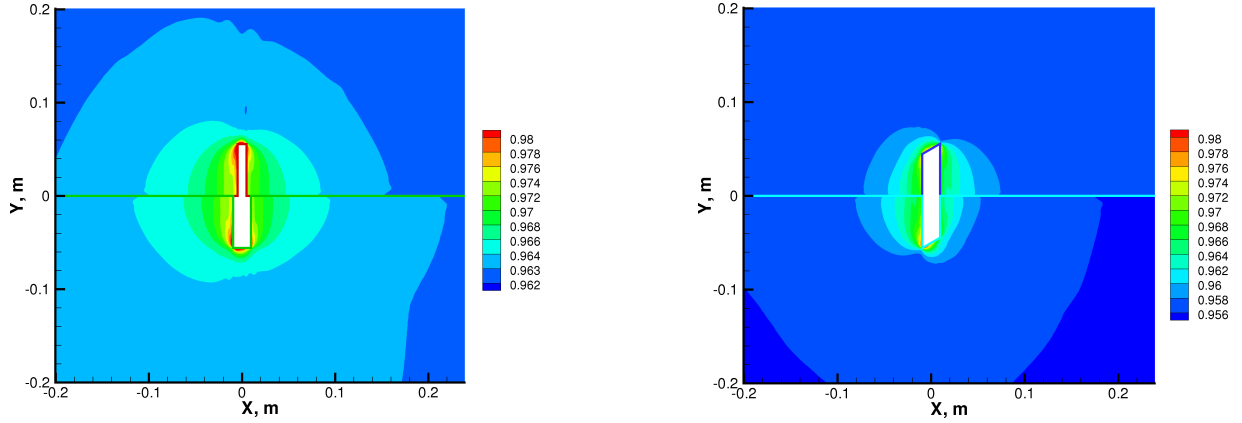


**FIGURE 2.** Pressure fields for  $\alpha = 90^\circ$ ,  $W = 0.5$  cm (left top),  $\alpha = 90^\circ$ ,  $W = 1.5$  cm (left bottom),  $\alpha = 60^\circ$ ,  $W = 1.5$  cm (right top) and  $\alpha = 120^\circ$ ,  $W = 1.5$  cm (right bottom).

**TABLE 1.** Pressure  $F_p$ , shear  $F_s$ , and total radiometric force  $F_{tot}$  for single vane configuration

Pressure	Force component (N)	$W = 0.5$ cm	$W = 1.5$ cm	$W = 1.5$ cm	$W = 1.0$ cm
		$\alpha = 90^\circ$	$\alpha = 90^\circ$	$\alpha = 60^\circ$	$\alpha = 120^\circ$
0.012	$F_p$	2.080E-06	2.080E-06	1.074E-06	
	$F_s$	-1.338E-09	-2.444E-09	5.056E-07	
	$F_{tot}$	2.079E-06	2.078E-06	1.580E-06	
0.066	$F_p$	9.430E-06	9.410E-06	5.474E-06	
	$F_s$	-4.126E-08	-7.560E-08	2.552E-06	
	$F_{tot}$	9.389E-06	9.334E-06	8.026E-06	
0.299	$F_p$	2.330E-05	2.320E-05	1.354E-05	
	$F_s$	-5.530E-07	-9.955E-07	9.677E-06	
	$F_{tot}$	2.275E-05	2.220E-05	2.322E-05	
0.596	$F_p$	2.800E-05	2.780E-05	1.002E-05	
	$F_s$	-1.377E-06	-2.416E-06	1.854E-05	
	$F_{tot}$	2.662E-05	2.538E-05	2.856E-05	
0.954	$F_p$	2.900E-05	2.860E-05	-2.200E-06	4.860E-05
	$F_s$	-2.312E-06	-3.948E-06	3.023E-05	-3.606E-05
	$F_{tot}$	2.669E-05	2.465E-05	2.803E-05	1.254E-05
1.2	$F_p$	2.800E-05	2.800E-05	-1.220E-05	
	$F_s$	-2.902E-06	-4.859E-06	3.879E-05	
	$F_{tot}$	2.510E-05	2.314E-05	2.659E-05	

an optimum angle for the radiometric force, and changing it slightly is expected to produce an even larger force. All this indicates that such a change in the vane geometry ( $\alpha < 90^\circ$ ) allows one to maintain the maximum radiometric force even for relatively large length-to-thickness ratios. This is especially important when considering multi-vane geometries, for which the radiometric force is maximized through etching or drilling holes in the mane vane, as discussed in the next section.

## MULTI-VANE CONFIGURATION

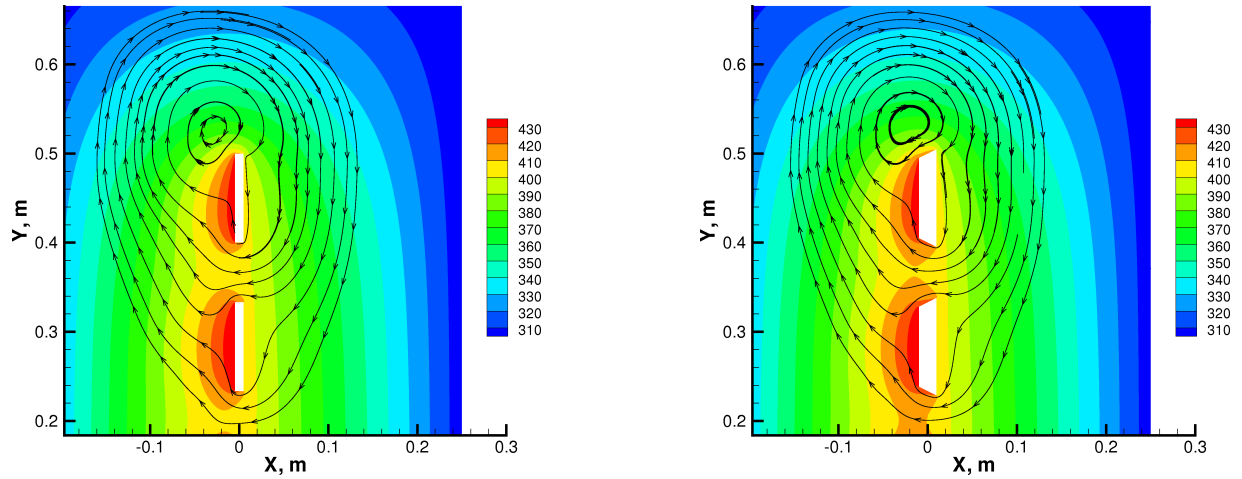
In an earlier work [10], feasibility of increasing the radiometric force through etching holes in the vane was investigated. In the cases of interest, the total area occupied by the radiometer was fixed, but the number of sub-vanes separated by gaps and the separation distance between them was varied to find the maximum radiometric force. It was found that a radiometer that consists of sub-vanes is much more efficient in terms of force production per radiometer mass than a solid plate radiometer that takes up the same effective area. Over an order of magnitude force increase was predicted. However, any further increase in efficiency was hampered by significant losses in net radiometric force caused by the shear on lateral surfaces of sub-vanes. This, along with the possibility of increasing the radiometric force

**TABLE 2.** Pressure, shear and total radiometric forces (N) for 7-vane configuration

Configuration	$W = 0.5 \text{ cm}$ $\alpha = 90^\circ$	$W = 1.0 \text{ cm}$ $\alpha = 90^\circ$	$W = 1.5 \text{ cm}$ $\alpha = 90^\circ$	$W = 1.0 \text{ cm}$ $\alpha = 76^\circ$	$W = 1.0 \text{ cm}$ $\alpha = 66.5^\circ$	$W = 1.0 \text{ cm}$ $\alpha = 116.5^\circ$	$W = 1.5 \text{ cm}$ $\alpha = 80.5^\circ$
$F_p$	5.090E-03	4.948E-03	4.806E-03	5.261E-03	5.420E-03	4.008E-03	5.153E-03
$F_s$	-8.560E-05	-1.148E-04	-1.312E-04	-2.320E-04	-3.370E-04	1.160E-04	-2.534E-04
$F_{tot}$	5.004E-03	4.833E-03	4.675E-03	5.029E-03	5.083E-03	4.124E-03	4.900E-03

in a stand-alone vane through the edge geometry modification, motivated the authors to analyze the results of such a modification in a multi-vane configuration. The computations were performed for a seven-vane geometry at a pressure of 1.5 Pa, where the radiometric force is near its maximum, and different values of the angle  $\alpha$  and vane thickness  $W$ .

Comparison of gas temperatures and streamlines for two different geometries is presented in Fig. 3 for 1.5 Pa. Only part of the computational domain near the two outer vanes is shown here in order to provide more detail. It is clear that the general flow structure is very similar. The thermal transpiration dominates the bulk flow motion, and the streamlines generally a directed from cold sides to hot sides of the vane. In both cases, there is also a smaller vortex near the hot side of the outermost vane. The large lateral sides of the  $\alpha = 66.5^\circ$  geometry result in somewhat higher temperatures between the vane for this case, although the gas temperatures near the hot and cold sides are nearly identical for  $\alpha = 90^\circ$  and  $\alpha = 66.5^\circ$ .

**FIGURE 3.** Temperature field and streamlines for  $\alpha = 90^\circ$ ,  $W = 0.5 \text{ cm}$  (left), and  $\alpha = 66.5^\circ$ ,  $W = 1 \text{ cm}$  (right).

The radiometric forces for all multi-vane cases under consideration are summarized in Table 2 for gas pressure of 1.5 Pa, where the force is near its maximum. Comparison of the three straight vane geometries with different thickness shows that the contribution of the shear force is much more pronounced than for the single-vane configuration considered earlier. The total decrease of the radiometric force due to shear increases from over 1.5% for the thinnest geometry to almost 3% for the thickest one. Note also that thicker vanes result in less efficient cold-to-hot gas recirculation, and thus reduce the pressure difference between the hot and cold sides. The total radiometric force decreases by about 7% when the vane thickness increases to 1.5 cm. Note that the force degradation would be significantly more pronounced if more vanes were used in this multi-vane geometry.

The change in the vane geometry allows for significant increase in the total radiometric force. With two values of  $\alpha < 90^\circ$  used in this work for  $W = 1.0 \text{ cm}$ , the  $\alpha = 66.5^\circ$  geometry produced a higher force (about 1.5% higher than for the thinner geometry). Interesting to note that in the slanted edge geometries, the shear force reduces the total force, opposite to what was observed for a single vane geometry. The shear force is negative since the angle  $\alpha$  is not small enough. The main reason for large total force in slanted geometries with  $\alpha < 90^\circ$  is significantly more efficient cold-to-hot gas flow, with the holes between the vanes acting in effects as small nozzles. The geometry with  $\alpha < 90^\circ$  is inefficient in terms of radiometric force, as also shown in the table. Even though the shear force becomes positive, and increases the total radiometric force, the pressure force is much smaller than for the corresponding straight edge geometry.

## CONCLUSIONS

The impact of vane edge shape on radiometric forces in single and multi-vane geometries was numerically evaluated by the solution of ES-BGK model kinetic equations in the range of pressures where the total radiometric force is near its maximum. The contribution of shear and pressure forces to the total force is analyzed. It was found that changing the edge geometry from straight to slanted, with the sharp edge at the cold side, helps offset the decrease in the force with increasing vane thickness. This is especially important for multi-vane geometries with relatively small separation between vanes. For such geometries, maximization of radiometric force per unit area (or per unit mass) requires increasing the number of vane with the corresponding decrease in size. The natural limitations of the length-to-thickness ratio may therefore be offset by an appropriate modification in the shape of the vane edges.

## ACKNOWLEDGMENTS

The work was supported in part by the Air Force Office of Scientific Research and the Propulsion Directorate of the Air Force Research Laboratory at Edwards Air Force Base California. The authors thank Ingrid Wysong and Dean Wadsworth for many fruitful discussions.

## REFERENCES

1. O. Reynolds, "On Certain Dimensional Properties of Matter in the Gaseous State," *Phil. Trans. R. Soc. of London* **170**, pp. 727–845 (1879).
2. J. C. Maxwell, "On stresses in rarified gases arising from inequalities of temperature," *Phil. Trans. R. Soc. of London* **170**, pp. 231–256 (1879).
3. A. Einstein, "Zur theorie der radiometerkräfte," *Zeitschrift für Physik* **27**, pp. 1–5 (1924).
4. H. E. Marsh, "Further experiments on the theory of the vane radiometer," *J. Opt. Soc. Amer.* **12**, pp. 135–147 (1926).
5. M. Scandurra, F. Iacopetti, and P. Colona, "Gas kinetic forces on thin plates in the presence of thermal gradients," *Physical Review E* **75**, 026308 (2007).
6. N. Selden, N. Gimelshein, S. Gimelshein, A. Ketsdever, "Analysis of accommodation coefficients of noble gases on aluminum surface with an experimental/computational method," *Physics of Fluids* **21**, pp. 073101-073101-8 (2009).
7. N. Selden, C. Ngalande, N. Gimelshein, S. Gimelshein, A. Ketsdever, "Origins of radiometric forces on a circular vane with a temperature gradient," *Journal of Fluid Mechanics* **634**, pp. 419–431 (2009).
8. N. Gimelshein, S. Gimelshein, N. Selden, A. Ketsdever, "Modeling of low-speed rarefied gas flows using a combined ES-BGK/DSMC approach," Submitted to *Vacuum*, July 2009.
9. N. Selden, C. Ngalande, S. Gimelshein, E. P. Muntz, A. Alexeenko, A. Ketsdever, "Area and edge effects in radiometric forces," *Physical Review E* **79**, 041201 (2009).
10. N. Gimelshein, S. Gimelshein, A. Ketsdever, N. Selden, "Impact of vane size and separation on radiometric forces for microactuation," Submitted to *Journal of Micromechanics and Microengineering*, Jan 2010.
11. G. A. Bird, *Molecular Gas Dynamics and the Direct Simulation of Gas Flows*, Clarendon Press, Oxford, 1994.
12. P. L. Bhatnagar, E. P. Gross, M. Krook, "A model for collision processes in gases I: Small amplitude processes in charged and neutral one-component systems," *Phys. Rev.* **94**, pp. 511–525 (1954).
13. L.H. Holway, "Numerical solutions for the BGK-model with velocity dependent collision frequency," in *Proc. IV Int. Symp. on Rarefied Gas Dynamics*, New York Academic Press, pp. 193-0215 (1966).
14. L. Mieussens, "Discrete-velocity models and numerical schemes for the Boltzmann-BGK equation in plane and axisymmetric geometries," *J. Comp. Phys.* **162**, pp. 429–466 (2000).